Crossing over is coupled to late meiotic prophase bivalent differentiation through asymmetric disassembly of the SC

Kentaro Nabeshima,[1] Anne M. Villeneuve,[1] and Monica P. Colaiácovo[1,2]

[1]Department of Developmental Biology and Department of Genetics, Stanford University School of Medicine, Stanford, CA 94305
[2]Department of Genetics, Harvard Medical School, Boston, MA 02115

Homologous chromosome pairs (bivalents) undergo restructuring during meiotic prophase to convert a configuration that promotes crossover recombination into one that promotes bipolar spindle attachment and localized cohesion loss. We have imaged remodeling of meiotic chromosome structures after pachytene exit in *Caenorhabditis elegans*. Chromosome shortening during diplonema is accompanied by coiling of chromosome axes and highly asymmetric departure of synaptonemal complex (SC) central region proteins SYP-1 and SYP-2, which diminish over most of the length of each desynapsing bivalent while becoming concentrated on axis segments distal to the single emerging chiasma. This and other manifestations of asymmetry along chromosomes are lost in synapsis-proficient crossover-defective mutants, which often retain SYP-1,2 along the full lengths of coiled diplotene axes. Moreover, a γ-irradiation treatment that restores crossovers in the *spo-11* mutant also restores asymmetry of SYP-1 localization. We propose that crossovers or crossover precursors serve as symmetry-breaking events that promote differentiation of subregions of the bivalent by triggering asymmetric disassembly of the SC.

Introduction

Structural remodeling of chromosomes is an integral feature of the meiotic program by which diploid germ cells generate haploid gametes (Page and Hawley, 2003). Chromosomes must acquire an organization that will promote both controlled DNA breakage and subsequent recombinational repair using the homologous chromosome as a repair partner to yield interhomologue crossovers; this organization includes meiosis-specific differentiation of chromosome axes and loading of proteins comprising the central region of the synaptonemal complex (SC), a structure linking the axes of aligned homologues. During later prophase, the SC disassembles and chromosomes undergo further structural remodeling to yield an organization in which homologues remain connected yet are oriented away from each other in a configuration that promotes their attachment to and segregation toward opposite poles of the meiosis I spindle. A crossover between the DNA molecules of homologues and cohesion between sister chromatids on both sides of the crossover together underpin this late prophase connection, known as the chiasma, that persists after SC disassembly. However, despite the central importance of chiasmata, we know very little about the processes of SC disassembly and chiasma emergence, or about how earlier events are coupled to these late prophase chromosome restructuring events.

The connections afforded by chiasmata necessitate a two-step loss of sister chromatid cohesion: partial loss of cohesion at meiosis I permits dissolution of chiasmata and homologue separation while maintaining the connections between sisters needed to permit congression and bipolar spindle attachment at meiosis II. In organisms with localized centromeres, two-step loss of cohesion is accomplished using protector proteins that localize to centromeres and shield centromeric cohesin from removal at meiosis I (Moore et al., 1998; Kitajima et al., 2004). However, this strategy is inadequate to explain how two-step loss of cohesion is accomplished in organisms such as *Caenorhabditis elegans* that do not have localized centromeres. Whereas diakinesis-stage bivalents in worms and mice are quite similar in their cytological appearance, during *C. elegans* meiosis either end of a given chromosome has the potential for kinetic activity, and the position of the crossover determines which region will retain cohesion and lead the way toward the pole at meiosis I (Albertson et al., 1997).

Correspondence to Anne M. Villeneuve: villen@cmgm.stanford.edu

Abbreviations used in this paper: DSB, double-strand break; IF, immunofluorescence; SC, synaptonemal complex.

The online version of this article includes supplemental material.

The Journal of Cell Biology, Vol. 168, No. 5, February 28, 2005 683–689
http://www.jcb.org/cgi/doi/10.1083/jcb.200410144

Here, we investigate the dynamic reorganization of chromosome structures during SC disassembly and chiasma emergence in *C. elegans*, where chromosome remodeling can be visualized in whole mount preparations that preserve temporal context and three-dimensional nuclear architecture. We show that SC disassembly occurs in a highly asymmetric fashion and is accompanied by coiling of chromosome axes. Furthermore, we provide insight into how a crossover can direct differentiation of subdomains of the late prophase bivalent. Our data support a model in which either crossovers or crossover precursors serve as symmetry-breaking events that trigger asymmetric disassembly of the SC and localized retention of SC central region components, which in turn guides the concentration of aurora-like kinase AIR-2 on the subregion of the bivalent where cohesin will be lost at meiosis I.

Results and discussion

Dynamic localization of meiosis-specific structural proteins and chromosome remodeling during SC disassembly and chiasma emergence

At the pachytene stage of meiotic prophase, when SC is present along the full lengths of parallel-aligned homologue pairs, immunofluorescence (IF) signals corresponding to SC central region protein SYP-1 are flanked by parallel tracks of DAPI-stained chromatin and exhibit essentially complete colocalization with IF signals corresponding to chromosome axis components HIM-3 and cohesin REC-8 (Zetka et al., 1999; Pasierbek et al., 2001; MacQueen et al., 2002; Nabeshima et al., 2004; Fig. 1). However, upon exit from pachynema, axis and central region proteins exhibit highly discordant behavior.

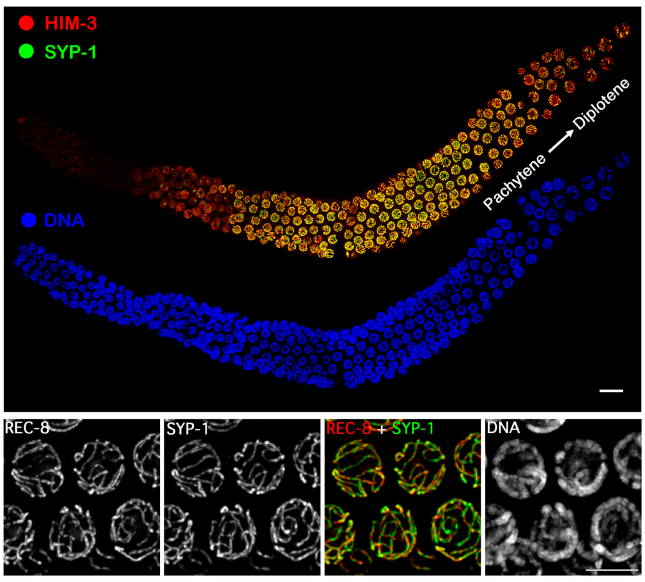

Figure 1. **Immunolocalization of axis and SC components during wild-type meiosis.** (Top) Whole mount germ line oriented with the distal premeiotic region at the left and the region of the pachytene–diplotene transition at the right. Bar, 10 μm. (Bottom) Pachytene nuclei exhibiting essentially full colocalization of SC central region protein SYP-1 and axis protein REC-8 between parallel tracks of DAPI-stained chromatin. Bar, 5 μm.

SC disassembly at the pachytene–diplotene transition is accompanied by a major transition in the organization of chromosome axes. REC-8 (Fig. 2) and HIM-3 (not depicted) continue to localize along the lengths of desynapsing chromosomes, but whereas REC-8 and HIM-3 signals appear as extended linear stretches in pachytene nuclei, this linear appearance gives way to a more convoluted appearance as nuclei enter diplonema. In a subset of diplotene nuclei, a coiled organization of chromosome axes can be clearly resolved (three-dimensional volume renderings in Fig. 2 D and Video 1, available at http://www.jcb.org/cgi/content/full/jcb200410144/DC1). Axis coiling coincides temporally with shortening of the end-to-end lengths of chromosomes that occurs at this stage, suggesting that coiling of preexisting axial structures may either contribute to or be a consequence of the chromosome shortening mechanism. Axis coiling during late meiotic prophase was observed previously in silver-stained preparations of rye and lily chromosomes (Fedotova et al., 1989; Stack, 1991); however, this is the first report of coiled axial structures during meiotic prophase visualized by imaging of specific molecular components.

In contrast to the continued association of axis proteins along the lengths of desynapsing chromosomes, IF signals for SC central region proteins SYP-1 and SYP-2 become greatly diminished over most of the chromosome lengths during this transition (Figs. 2 A and 3). SYP-1 continues to colocalize with axis components, but becomes concentrated over a limited subdomain of axis staining. Evidence of asymmetry is first seen in late pachynema, after disappearance of RAD-51 foci (indicating progression of recombination past the strand exchange step), as unevenness in the intensity of SYP-1,2 signals along the length of a still-synapsed homologue pair (Fig. 2, B and C). By mid-diplonema, six robust, discrete SYP-1,2 stretches are readily resolved in each nucleus, corresponding to the number of homologue pairs in the diploid chromosome complement; analysis of three-dimensional image stacks reveals that SYP-1,2 become concentrated preferentially on a single portion of each bivalent. Diplotene bivalents typically have a Y- or X-shaped appearance (Fig. 2 D and Videos 1 and 2, available at http://www.jcb.org/cgi/content/full/jcb200410144/DC1). Y-shaped bivalents have two symmetric longer axis stretches, corresponding to homologue segments that are disassociating from each other, and one shorter stretch of axis staining, corresponding to a region in which the two homologue axes are still coaligned; SYP-1 colocalization with this shorter stretch likely corresponds to a remnant of the disassembling SC. X-shaped bivalents have two symmetric long axis stretches and two symmetric short axis stretches, corresponding to separating segments of homologues, joined by a short region in which homologues are still closely juxtaposed; SYP-1 is concentrated on this region and on the shorter arms of the X. Based on such images, we conclude that SYP-1,2 become concentrated in the vicinity of and toward one side of the single emerging chiasma.

IF signals from regions of SYP-1 concentration at diplonema appear brighter than SYP-1 signals seen along the lengths of mid-pachytene bivalents (Fig. 2 A and not depicted). This increased intensity may reflect an increased local SYP-1

concentration resulting from the combined effects of localized retention and consolidation of signals through chromosome condensation. Alternatively, it might reflect recruitment of SYP-1 departing from one region of the chromosomes to the regions where it is being retained.

Fig. 2 E shows bivalents that have undergone a further transition from the diplotene organization to the highly compact diakinesis organization. Chiasmata are clearly evident, and DAPI staining shows that sister chromatids are substantially resolved as separate entities. Axis proteins are detected as a cross localized at the interface between sister chromatids and centered on the chiasma. Bivalents are usually asymmetric, reflecting the fact that most autosome pairs enjoy a single crossover at an off-center position, within 25–35% of the chromosome length from an end (Albertson et al., 1997). At early to mid-diakinesis, SYP-1 and SYP-2 are concentrated mainly on the short axis of the bivalent, a region now operationally defined as distal to the chiasma. At this stage, SYP-1,2 are no longer part of a structure linking the axes of coaligned homologues, as homologous chromosome segments have lost their parallel alignment and are now oriented away from each other, adopting diametrically opposed positions within the bivalent. By late diakinesis, SYP-1,2 are no longer detected on the bivalent, but the cross-shaped localization of axis components remains robust (Zetka et al., 1999; Pasierbek et al., 2001; MacQueen et al., 2002; Colaiácovo et al., 2003).

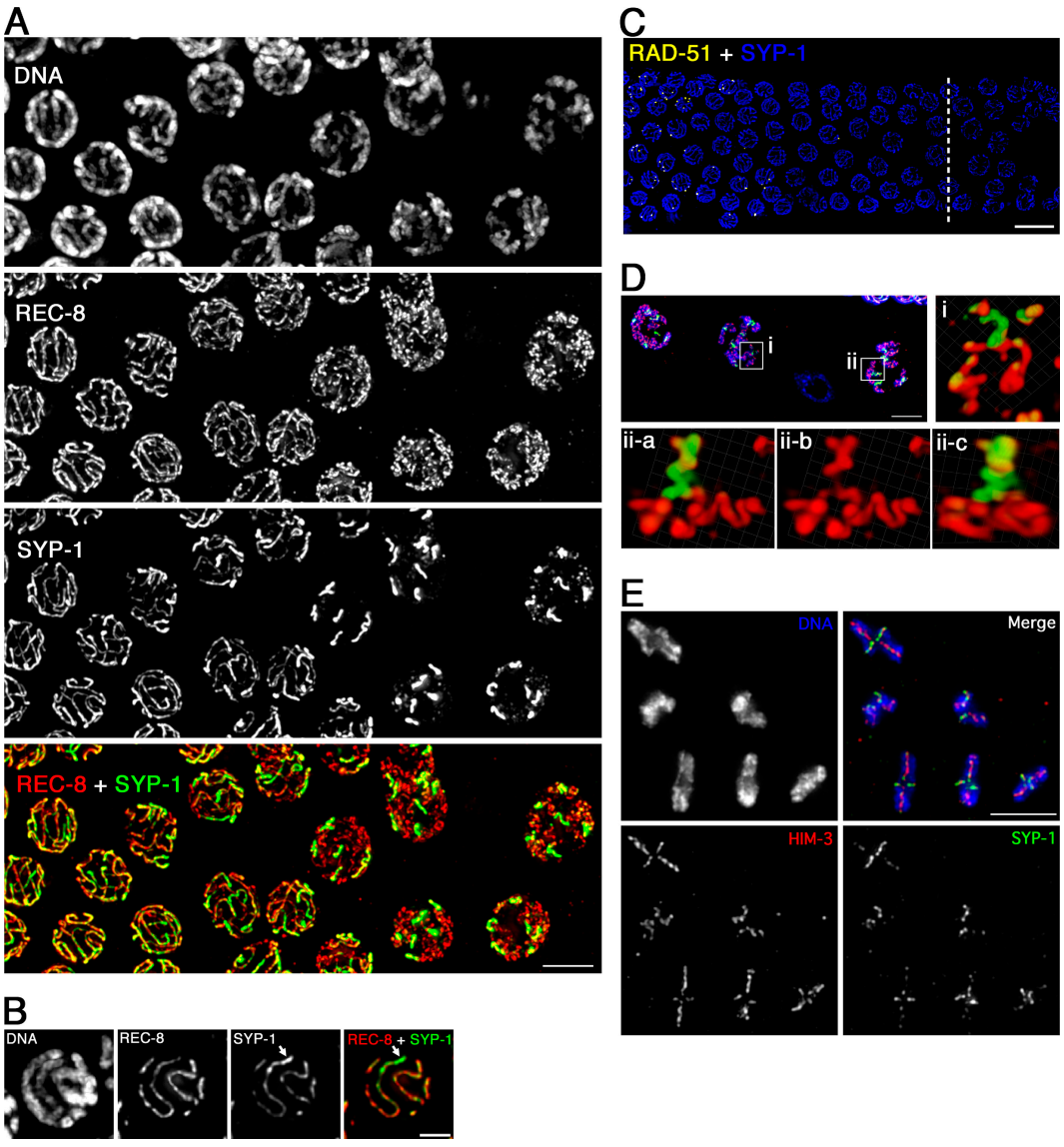

Figure 2. **Chromosome reorganization after pachytene exit.** See text for description. (A) Immunolocalization of REC-8 and SYP-1 at the pachytene–diplotene transition; late pachytene nuclei are at the left, diplotene at the right. Bar, 5 μm. (B) Projection halfway through a late pachytene nucleus showing unevenness in intensity of SYP-1 signal along bivalent (arrow). Bar, 2 μm. (C) Position of nuclei showing SYP-1 asymmetry (right side of a dashed line) relative to disappearance of RAD-51 foci. Bar, 10 μm. (D) Volume renderings of individual diplotene bivalents. Red, α-REC-8; green, α-SYP-1; blue, DAPI. i, X-shaped bivalent; ii-a–c, Y-shaped bivalent shown from two different angles. Bar, 5 μm. Videos 1 and 2 (available at http://www.jcb.org/cgi/content/full/jcb200410144/DC1) show rotating images of these bivalents. (E) Complete complement of bivalents from a single oocyte nucleus at early/mid-diakinesis. Bar, 5 μm.

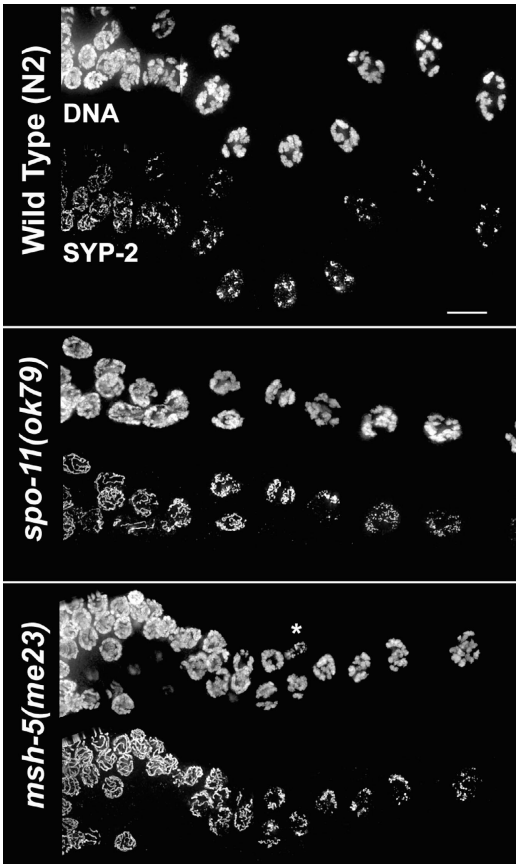

Figure 3. **Immunolocalization of SYP-2 after pachytene exit.** α-SYP-2 staining and DAPI-stained chromatin in wild-type, *spo-11*, and *msh-5* germ lines; portions shown extend from the region of pachytene exit (left) through late diplonema/early diakinesis (right). *, somatic nucleus. Bar, 10 μm.

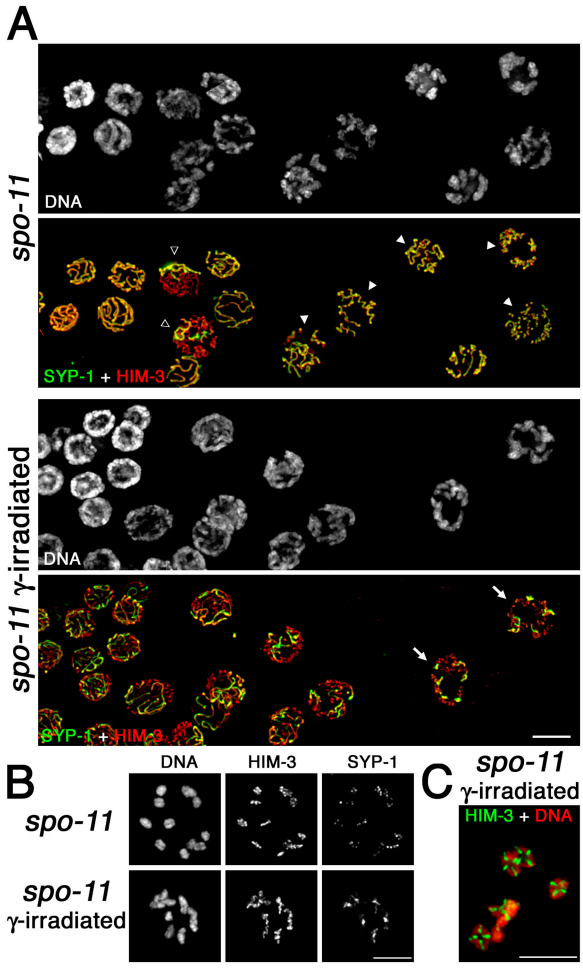

Figure 4. **Localization of SYP-1 and HIM-3 after pachytene exit in untreated and γ-irradiated *spo-11* mutants.** (A) Portions of germ lines extend from late pachynema (left) through mid/late diplonema (right). Closed arrowheads indicate diplotene nuclei in which SYP-1 is retained along the lengths of coiled axes; open arrowheads indicate nuclei in which SYP-1 has been lost from the majority of the chromosomes but is retained on some chromosomes; arrows indicate nuclei in which each desynapsing bivalent retains a single robust stretch of SYP-1, reflecting restoration of orderly asymmetric departure of SYP-1 by γ-irradiation. (B, top) Mid-diakinesis oocyte from an untreated *spo-11* worm showing lack of chiasmata and SYP-1 distributed along the lengths of the axes. (bottom) Late diplotene oocyte from a γ-irradiated *spo-11* worm showing SYP-1 concentrated on a region of each bivalent in the vicinity of and/or distal to the emerging chiasma. (C) Late diakinesis oocyte from a γ-irradiated *spo-11* worm showing restoration of chiasmata. Bars, 5 μm.

Asymmetric SC disassembly is coupled to meiotic recombination

As the aforementioned events suggested a coupling between chiasma formation and asymmetric SC disassembly, we investigated SC disassembly in the absence of crossing over. We examined the *spo-11(ok79)* mutant (Dernburg et al., 1998), which assembles SC between fully aligned homologues but lacks the double-strand break (DSB)–forming enzyme that initiates recombination.

The *spo-11* mutant is severely impaired in achieving orderly asymmetric departure of SYP-1,2 from meiotic prophase chromosomes (Figs. 3 and 4 A). This is particularly evident at diplonema, when SYP-1,2 fail to become concentrated to a single short stretch per homologue pair. Instead, *spo-11* diplotene nuclei exhibit several types of anomalies. In some nuclei, SYP-1 is retained along the full lengths of coiled axes, and DAPI-staining shows that the homologues are still largely synapsed; this differs from wild-type meiosis, where axis coiling is usually seen only in nuclei exhibiting extensive desynapsis. In other nuclei, SYP-1,2 have been lost from the entire lengths of most of the chromosomes within the nucleus, but a few bright chromosome-associated SYP-1,2 signals are present; the appearance of the HIM-3 signals and DAPI-stained chromatin in such nuclei indicates that homologues are largely desynapsed. Finally, some nuclei exhibit a mixture of these two phenotypes. In summary, meiotic chromosomes in the *spo-11* mutant have not lost either the ability to retain or to eject SYP-1,2; rather, they have lost the capacity to coordinate retention and loss in a manner that results in reliable asymmetric differentiation of chromosomal subdomains.

Failure to differentiate distinct subdomains is also evident at early/mid diakinesis in the *spo-11* mutant (Figs. 4 B and 5 A). Chromosomes are fully resolved into 12 univalents, indicating eventual desynapsis, and SYP-1 signals are found distributed along the entire lengths of the axes rather than being concentrated on axis subdomains as in wild type. SYP-1 signal intensities are variable among different univalents within a given nucleus, suggesting a stochastic aspect to SYP-1 localization.

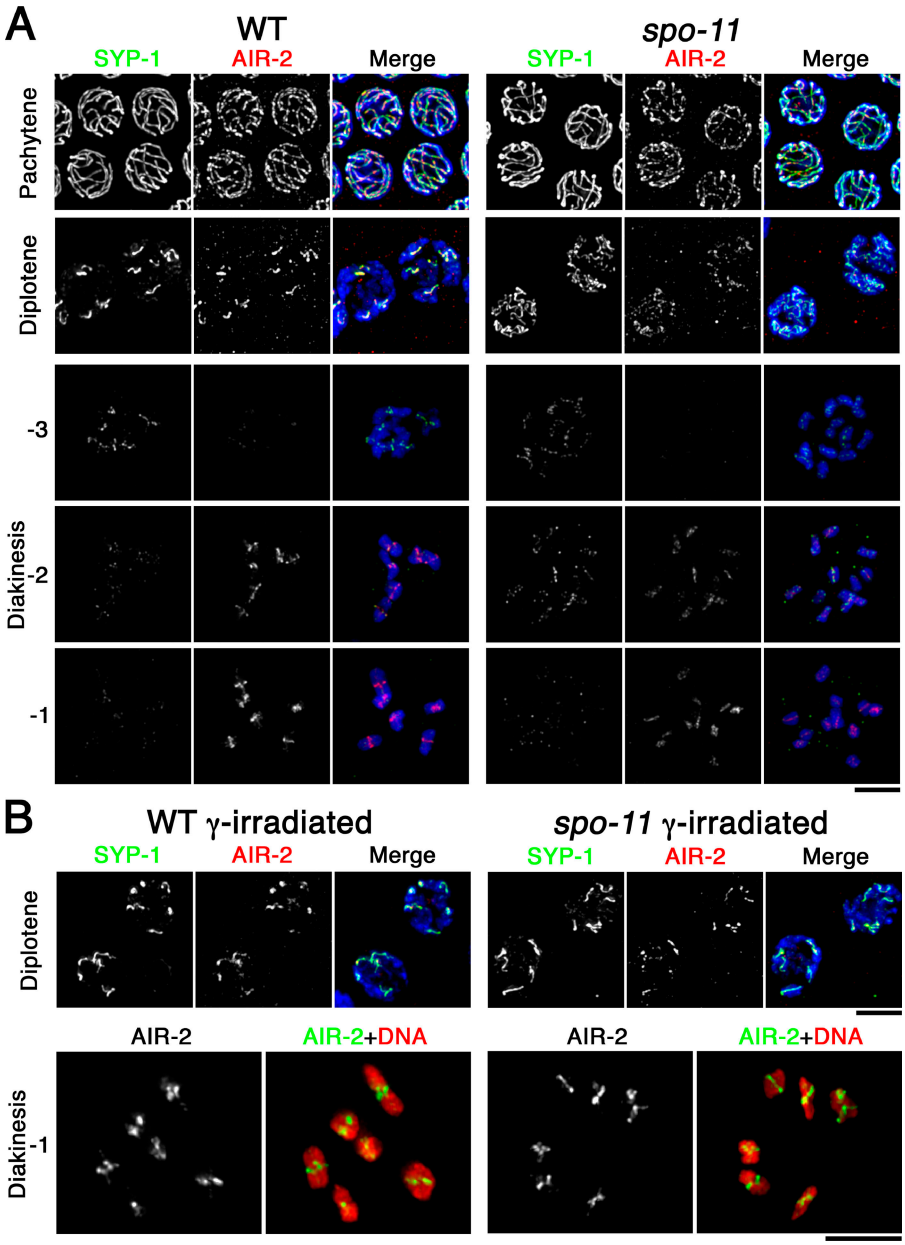

Figure 5. **Dynamic localization of SYP-1 and AIR-2.** (A) Immunolocalization of SYP-1 and AIR-2 in wild-type and *spo-11* nuclei at the indicated stages. For diakinesis nuclei, −3, −2, and −1 indicate position relative to the spermatheca, with the oocyte in the −1 position (closest to the spermatheca) being the most mature. In A and B, detection thresholds for α-AIR-2 signals were lower for the pachytene and diplotene panels than for the diakinesis panels to permit imaging of both the lower levels of chromosome-associated AIR-2 at the earlier stages and the subchromosomal localization of the higher levels of AIR-2 in late diakinesis. DAPI-stained chromatin is shown in blue in the merged images. (B) SYP-1 and AIR-2 localization after γ-irradiation. Bars, 5 μm.

As DNA breaks induced by γ-irradiation can bypass the requirement for SPO-11, rescuing the crossover and chiasma formation defects in a *spo-11* mutant (Dernburg et al., 1998), we tested whether or not γ-irradiation could also restore asymmetry of SYP-1 departure. Fig. 4 (A and B) and Fig. 5 B show that asymmetry is indeed substantially restored in the *spo-11* mutant after γ-irradiation. In irradiated *spo-11* worms, we observed diplotene nuclei with six robust SYP-1 stretches, each concentrated over a limited subset of axis staining corresponding to the still-synapsed regions of the desynapsing bivalents. Restoration of localized SYP-1 retention by γ-irradiation indicates that some aspect of the recombination event by itself, rather than the SPO-11 protein, is responsible for eliciting asymmetry in SC disassembly.

In both irradiated wild-type and *spo-11* worms, some late prophase bivalents did not appear completely normal (Fig. 5 B and not depicted). Diplotene SYP-1 stretches appeared more variable in length than in unirradiated wild-type, and some late diplotene bivalents had a more symmetrical Y-shaped structure than is typical for wild-type meiosis. Furthermore, in some diakinesis bivalents the homologues were connected at extreme terminal positions. Such abnormalities likely reflect formation of crossovers at unusual chromosomal locations, as noted in Dernburg et al. (1998).

We also examined chromosome dynamics following pachytene exit in *msh-5(me23)* and *him-14/msh-4(it21)* mutants, which form DSBs and load RAD-51 but fail to complete initiated recombination events as crossovers (Zalevsky et al., 1999; Kelly et al., 2000; Colaiácovo et al., 2003). These mutants are also highly defective in achieving orderly asymmetric disassembly of SC, failing to concentrate SYP-1,2 to a single robust stretch per bivalent (Fig. 3 and not depicted).

This result indicates that DSB formation and RAD-51 loading are not sufficient to trigger orderly asymmetric SC disassembly.

Together, our observations suggest that crossovers (or precursor events in the crossover pathway) serve as symmetry-breaking events during differentiation of meiotic prophase bivalents, triggering asymmetric SC disassembly and localized retention of SC central region proteins. We suggest that the single maturing or completed crossover per homologue pair subdivides the bivalent into two separate domains. Because crossovers usually occur at clearly off-center positions, these domains will be inherently unequal in length. We can envision how this asymmetry in length might set up an unstable equilibrium between association and dissociation of SYP-1,2 modules that results in localized retention and/or concentration of SYP-1,2 on the shorter segment: if the initial probability of dissociation increases with distance from the crossover, and if dissociation increases the likelihood of dissociation in adjacent intervals (e.g., by removing constraints that inhibit changes in chromosome geometry driven by chromatin expansion forces [Kleckner et al., 2004]), the observed concentration of SYP-1,2 on the shorter segment is expected to ensue.

SYP-1 guides AIR-2 localization during bivalent differentiation

The subregion of the bivalent to which SYP-1,2 localize from diplonema through mid-diakinesis corresponds to the region where Aurora-like kinase AIR-2 will become localized at the end of diakinesis (Kaitna et al., 2002; Rogers et al., 2002) and where REC-8 will be lost at the metaphase to anaphase transition of meiosis I (Pasierbek et al., 2001). Moreover, AIR-2 can phosphorylate REC-8 in vitro and is required for loss of REC-8 distal to the chiasma at meiosis I (Rogers et al., 2002). As asymmetric SC disassembly and localized SYP-1 retention after SC disassembly presage these later aspects of bivalent differentiation, we investigated the connection between SYP-1 and AIR-2 localization. Although earlier papers had suggested that AIR-2 first localizes to meiotic chromosomes at late diakinesis (in the −1 or −2 oocyte), our imaging and that of Chan et al. (2004) revealed much earlier chromosomal localization of AIR-2. We detected AIR-2 colocalized with SYP-1 during pachynema and diplonema, and dynamic changes in AIR-2 localization during the transition between these stages closely paralleled those of SYP-1 (Fig. 5). Chromosomal localization of AIR-2 in pachytene and diplotene regions of the germline is lost in *syp-1* mutants (unpublished data), indicating that AIR-2 localization at these stages is SYP-1 dependent. Furthermore, AIR-2 localization tracked with SYP-1 in pachytene through diplotene stages both in the unirradiated *spo-11* mutant and in γ-irradiated *spo-11* mutant nuclei in which SYP-1 asymmetry had been restored. Together these observations suggest that pachytene and diplotene localization of SYP-1 dictates where AIR-2 will be localized at these stages.

AIR-2 staining diminished to nearly undetectable levels in early diakinesis, and in wild-type worms robust AIR-2 staining was later detected in the −1 and −2 oocytes, concentrated at the midbivalents on the short axis segments distal to the chiasmata (Kaitna et al., 2002; Rogers et al., 2002). In contrast, AIR-2 staining in the −1 and −2 oocytes of *spo-11* mutants was less intense, was variable among different univalents within nuclei, and was distributed along the length of the univalents. Restoration of chiasmata by γ-irradiation in *spo-11* mutants was accompanied by restoration of robust AIR-2 staining, usually concentrated at the midbivalent on the shorter axis segments (Fig. 5 B). These observations support a model in which asymmetry in SYP-1 localization is an early feature of asymmetric bivalent differentiation that in turn guides a later feature of bivalent differentiation, concentration of AIR-2 to the region now defined as distal to the chiasma.

Conclusions

Our observations support a model in which maturing or completed crossovers serve as symmetry-breaking events in meiotic prophase chromosome differentiation, triggering asymmetry in the departure/retention of SC central region proteins during chromosome remodeling at the pachytene–diplotene transition. Asymmetric differentiation of meiotic prophase bivalents occurs in parallel with axis coiling (this work) and condensin-mediated processes that promote chromosome compaction and sister chromatid resolution (Chan et al., 2004). We further propose that asymmetry in localization of SC central region components, directed by the crossover, in turn directs where AIR-2 will become concentrated at the end of prophase, thereby allowing the position of the crossover to dictate the region of cohesin loss at meiosis I.

Materials and methods

Immunostaining was performed as described in Nabeshima et al. (2004) for Figs. 1, 2, 4, and 5 and as described in Colaiácovo et al. (2003) for Fig. 3, using whole-mount dissected germ lines from adult hermaphrodites 21–24 h post-L4 larval stage (except for Fig. 2 E, where a coverslip placed over the whole mount was tapped gently with a pencil tip during fixation to increase spacing between bivalents). For γ-irradiation experiments, late L4 worms were exposed to 5,000 rad and their germ lines were dissected and fixed 19 h later. The following primary antibodies were used at the indicated dilutions: rabbit α-HIM-3 (Zetka et al., 1999; obtained from M. Zetka, McGill University, Montreal, Canada; 1:200), rabbit α-REC-8 (Pasierbek et al., 2001; obtained from J. Loidl, University of Vienna, Vienna, Austria; 1:100), guinea pig α-SYP-1 (MacQueen et al., 2002; 1:100), rabbit α-SYP-2 (Colaiácovo et al., 2003; 1:200), and rabbit α-AIR-2 (Schumacher et al., 1998; obtained from J. Schumacher, University of Texas MD Anderson Cancer Center, Houston, TX; 1:100). Secondary antibodies used were FITC anti–rabbit, Cy3 anti–guinea pig, and Cy3 anti-rabbit (Jackson ImmunoResearch Laboratories) each at 1:200 or Alexa 488 anti–rabbit and Alexa 555 anti–guinea pig (Molecular Probes) at 1:400. Mounting medium used was VECTASHIELD H-1000 (Vector Laboratories).

Images were obtained using an IX-70 microscope (Olympus) and recorded with a cooled CCD camera (model CH350; Roper Scientific) under control of the DeltaVision system with SoftWoRx software (Applied Precision). A PlanApo 60× lens (NA 1.4) was used for images in Figs. 1, 2, 4, and 5; a U-APO 40× lens (NA 0.65–1.35) was used for Fig. 3. Optical sections were collected at 0.20-μm increments and deconvolved using a conservative algorithm with 15 iterations. Except where noted, images are projections of data stacks encompassing entire nuclei generated using Quick Projection in the max intensity mode. Volume renderings in Fig. 2 B were generated using the Volocity Visualization software (Improvision Inc.) with a correction for optical distortion in the z-axis as described in Blower et al. (2002).

Online supplemental material
Videos 1 and 2 are QuickTime movies showing rotating images of the three-dimensional volume renderings of diplotene bivalents from Fig. 2 D. Online supplemental material is available at http://www.jcb.org/cgi/content/full/jcb200410144/DC1.

We thank M. Zetka, J. Loidl, and J. Schumacher for reagents and J. Bessler, N. Miley, and K. Reddy for comments on the manuscript.

This work was supported by National Institutes of Health grant R01GM53804 to A.M. Villeneuve, by training funds from Osaka University to K. Nabeshima, and by National Research Service Award Fellowship F32HD41329 and institutional support from Harvard Medical School to M.P. Colaiácovo.

Submitted: 31 October 2004
Accepted: 14 January 2005

References

Albertson, D.G., A.M. Rose, and A.M. Villeneuve. 1997. Chromosome organization, mitosis, and meiosis. *In C. elegans* II. D.L. Riddle, T. Blumenthal, B.J. Meyer, and J.R. Priess, editors. Cold Spring Harbor Laboratory Press, Plainview, NY. 47–78.

Blower, M.D., B.A. Sullivan, and G.H. Karpen. 2002. Conserved organization of centromeric chromatin in flies and humans. *Dev. Cell.* 2:319–330.

Chan, R.C., A.F. Severson, and B.J. Meyer. 2004. Condensin restructures chromosomes in preparation for meiotic divisions. *J. Cell Biol.* 167:613–625.

Colaiácovo, M.P., A.J. MacQueen, E. Martinez-Perez, K. McDonald, A. Adamo, A. La Volpe, and A.M. Villeneuve. 2003. Synaptonemal complex assembly in *C. elegans* is dispensable for loading strand-exchange proteins but critical for proper completion of recombination. *Dev. Cell.* 5:463–474.

Dernburg, A.F., K. McDonald, G. Moulder, R. Barstead, M. Dresser, and A.M. Villeneuve. 1998. Meiotic recombination in *C. elegans* initiates by a conserved mechanism and is dispensable for homologous chromosome synapsis. *Cell.* 94:387–398.

Fedotova, Y.S., O.L. Kolomiets, and Y.F. Bogdanov. 1989. Synaptonemal complex transformations in rye microsporocytes at the diplotene stage of meiosis. *Genome.* 32:816–823.

Kaitna, S., P. Pasierbek, M. Jantsch, J. Loidl, and M. Glotzer. 2002. The aurora B kinase AIR-2 regulates kinetochores during mitosis and is required for separation of homologous chromosomes during meiosis. *Curr. Biol.* 12:798–812.

Kelly, K.O., A.F. Dernburg, G.M. Stanfield, and A.M. Villeneuve. 2000. *Caenorhabditis elegans* msh-5 is required for both normal and radiation-induced meiotic crossing over but not for completion of meiosis. *Genetics.* 156:617–630.

Kitajima, T.S., S.A. Kawashima, and Y. Watanabe. 2004. The conserved kinetochore protein shugoshin protects centromeric cohesion during meiosis. *Nature.* 427:510–517.

Kleckner, N., D. Zickler, G.H. Jones, J. Dekker, R. Padmore, J. Henle, and J. Hutchinson. 2004. A mechanical basis for chromosome function. *Proc. Natl. Acad. Sci. USA.* 101:12592–12597.

MacQueen, A.J., M.P. Colaiácovo, K. McDonald, and A.M. Villeneuve. 2002. Synapsis-dependent and -independent mechanisms stabilize homolog pairing during meiotic prophase in *C. elegans. Genes Dev.* 16:2428–2442.

Moore, D.P., A.W. Page, T.T. Tang, A.W. Kerrebrock, and T.L. Orr-Weaver. 1998. The cohesion protein MEI-S332 localizes to condensed meiotic and mitotic centromeres until sister chromatids separate. *J. Cell Biol.* 140:1003–1012.

Nabeshima, K., A.M. Villeneuve, and K.J. Hillers. 2004. Chromosome-wide regulation of meiotic crossover formation in *Caenorhabditis elegans* requires properly assembled chromosome axes. *Genetics.* 168:1275–1292.

Page, S.L., and R.S. Hawley. 2003. Chromosome choreography: the meiotic ballet. *Science.* 301:785–789.

Pasierbek, P., M. Jantsch, M. Melcher, A. Schleiffer, D. Schweizer, and J. Loidl. 2001. A *Caenorhabditis elegans* cohesion protein with functions in meiotic chromosome pairing and disjunction. *Genes Dev.* 15:1349–1360.

Rogers, E., J.D. Bishop, J.A. Waddle, J.M. Schumacher, and R. Lin. 2002. The aurora kinase AIR-2 functions in the release of chromosome cohesion in *Caenorhabditis elegans* meiosis. *J. Cell Biol.* 157:219–229.

Schumacher, J.M., A. Golden, and P.J. Donovan. 1998. AIR-2: An Aurora/Ipl1-related protein kinase associated with chromosomes and midbody microtubules is required for polar body extrusion and cytokinesis in *Caenorhabditis elegans* embryos. *J. Cell Biol.* 143:1635–1646.

Stack, S.M. 1991. Staining plant cells with silver. II. Chromosome cores. *Genome.* 34:900–908.

Zalevsky, J., A.J. MacQueen, J.B. Duffy, K.J. Kemphues, and A.M. Villeneuve. 1999. Crossing over during *Caenorhabditis elegans* meiosis requires a conserved MutS-based pathway that is partially dispensable in budding yeast. *Genetics.* 153:1271–1283.

Zetka, M.C., I. Kawasaki, S. Strome, and F. Muller. 1999. Synapsis and chiasma formation in *Caenorhabditis elegans* require HIM-3, a meiotic chromosome core component that functions in chromosome segregation. *Genes Dev.* 13:2258–2270.